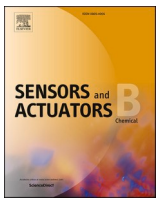
Sensors & Actuators: B. Chemical 381 (2023) 133433



Contents lists available at ScienceDirect

Sensors and Actuators: B. Chemical

journal homepage: www.elsevier.com/locate/snb





RT-RPA-Cas12a-based assay facilitates the discrimination of SARS-CoV-2 variants of concern

Guiyue Tang [a,1], Zilong Zhang [b,1], Wei Tan [a,1], Fei Long [a], Jingxian Sun [a], Yingying Li [a], Siwei Zou [a], Yujiao Yang [c], Kezhu Cai [a,d], Shenwei Li [b], Zhiyi Wang [b], Jiakun Liu [a], Guobing Mao [a], Yingxin Ma [a], Guo-Ping Zhao [a,c,e,*], Zhen-Gan Tian [b,**], Wei Zhao [a,**]

[a] CAS Key Laboratory of Quantitative Engineering Biology, Shenzhen Institute of Synthetic Biology, Shenzhen Institutes of Advanced Technology, Chinese Academy of Sciences, Shenzhen 518055, China
[b] Shanghai International Travel Healthcare Center, Shanghai Customs District P. R. China, Shanghai 200335, China
[c] CAS Key Laboratory of Synthetic Biology, CAS Center for Excellence in Molecular Plant Sciences, Chinese Academy of Sciences, Shanghai 200032, China
[d] School of Engineering, Southern University of Science and Technology, Shenzhen 518055, China
[e] Department of Microbiology and Microbial Engineering, School of Life Sciences, Fudan University, Shanghai 200433, China

ARTICLE INFO

Keywords:
SARS-CoV-2
Variant of concern
RRCd
Point-of-care testing
CRISPR

ABSTRACT

Timely and accurate detection of SARS-CoV-2 variants of concern (VOCs) is urgently needed for pandemic surveillance and control. Great efforts have been made from a mass of scientists in increasing the detection sensitivity and operability, and reducing the turn-around time and cost. Here, we report a nucleic acid testing-based method aiming to detect and discriminate SARS-CoV-2 mutations by combining RT-RPA and CRISPR-Cas12a detecting assays (RRCd). With a detection limit of 10 copies RNA/reaction, RRCd was validated in 194 clinical samples, showing 89% positive predictive agreement and 100% negative predictive agreement, respectively. Critically, using specific crRNAs, representatives of single nucleotide polymorphisms and small deletions in SARS-CoV-2 VOCs including N501Y, T478K and ΔH69-V70 were discriminated by RRCd, demonstrating 100% specificity in clinical samples with $C_t < 33$. The method completes within 65 min and could offer visible results without using any electrical devices, which probably facilitate point-of-care testing of SARS-CoV-2 variants and other epidemic viruses.

1. Introduction

The pandemic of COVID-19 has caused 623.8 million infections and 6.5 million deaths as of October 22th 2022 (https://covid19.who.int/table). The pathogen of this pandemic, SARS-CoV-2, has undergone rapid and constant mutations in the process of transmissions, bringing worldwide uncertainty to the diagnostics, vaccine effectiveness and therapeutics [1].

Since November 2020, generally five rapidly expanding SARS-CoV-2 lineages have been discovered and designated as variants of concern (VOCs), *i.e.*, the Alpha, Beta, Gamma, Delta, and Omicron [2]. Besides the current Omicron, among these lineages, the Alpha and Delta VOCs were dominant in frequency over a relatively long period of time. With gradual resumption of air travel, customs, and ports, previously isolated countries and regions are now easily exposed to the SARS-CoV-2 variants. These variants, either with higher infectivity or increased pathogenicity, could trigger outbreak waves unless they are detected timely and accurately [1,2].

Although quantitative reverse transcription PCR (RT-qPCR) performs as a gold standard for the SARS-CoV-2 detection, it is barely used to genotype the SARS-CoV-2 VOCs due to its limitations as an amplicon-based method. The current method is heavily based on in-depth whole-genome sequencing, which not only relies on bulk instruments and trained personnel but is also time-consuming and with relatively high cost [3,4]. A recent study showed that the multiplex qPCR could discriminate some of SARS-CoV-2 VOCs by targeting specific small

* Corresponding author at: CAS Key Laboratory of Quantitative Engineering Biology, Shenzhen Institute of Synthetic Biology, Shenzhen Institutes of Advanced Technology, Chinese Academy of Sciences, Shenzhen 518055, China.
** Corresponding authors.
E-mail addresses: gpzhao@sibs.ac.cn (G.-P. Zhao), tianzhenganciq@163.com (Z.-G. Tian), wei.zhao1@siat.ac.cn (W. Zhao).
[1] These authors contributed equally.

https://doi.org/10.1016/j.snb.2023.133433
Received 2 November 2022; Received in revised form 9 December 2022; Accepted 4 January 2023
Available online 26 January 2023
0925-4005/© 2023 The Authors. Published by Elsevier B.V. This is an open access article under the CC BY license (http://creativecommons.org/licenses/by/4.0/).

deletions [5]. However, this method is insensitive to the point mutations and other developing variations in SARS-CoV-2. Similarly, antigen-based detection assays have lower sensitivity than RT-qPCR and have not been reported to identify SARS-CoV-2 VOCs yet [6].

CRISPR-based technology was proven to have unique advantages in molecular diagnosis over the conventional PCR methods in terms of specificity and operability [7–9]. Two CRISPR-based COVID-19 diagnostic methods, DETECTR and SHERLOCK, have been developed using either Cas12a or Cas13a, with the characteristics of rapid, ultrasensitive and easy-to-implement [10,11]. Moreover, CRISPR assays such as RAY and PAM-targeting methods were employed to identify the point mutations in SARS-CoV-2 due to the high specificity of Cas/guide-RNA recognition [4,12,13]. Nevertheless, the relying on well-designed ligation probes or guide RNAs somehow limited the targeting capability of these methods to diverse mutation sites. Recently, CRISPR-based point-of-care tests (POCT) of SARS-CoV-2 were reported [14,15]. The methods provided visual readout using minimal fluorescent instruments and could identify multiple SARS-CoV-2 VOCs, among the synthetic samples though. Hence, significant efforts are still needed in respect to improving the detection sensitivity and validating the methods with clinical samples.

Here, we report a method combining reverse transcription-recombinase polymerase amplification (RT-RPA) and CRISPR-Cas12a technology based on our HOLMES test platform [16,17], aiming to detect and discriminate SARS-CoV-2 mutations. By exchanging the crRNA sequences, the method (RRCd) achieved to discriminate the well-known single nucleotide polymorphisms (SNPs) of N501Y and T478K as well as the small deletion of ΔH69-V70, corresponding to the major VOCs such as the Alpha and Omicron. RRCd was validated in 194 clinical samples after being systematic optimization, showing 89% positive predictive agreement and 100% negative predictive agreement, respectively. The results of RRCd could be visualized within about one hour. Moreover, due to using RT-RPA-Cas12a technical route and specific sample release reagents, all procedures of RRCd could be carried out at 37 °C and with no need for RNA extraction and purification, which is very conducive to the development of POCT products.

2. Experiments

2.1. Reverse transcription and recombinase polymerase amplification (RT-RPA)

A 20 μl volume-basic RT reaction mixture was used with 1 × RT buffer (Cat# EP0442, Thermo Scientific), 10 μl RNA template, 200 U RevertAid reverse transcriptase (Cat# EP0442, Thermo Scientific), 1.25 μM RT-RPA forward and reverse primer mix, 1 mM dNTP mix (Cat# P031–01, Vazyme, Nanjing, China), and 20 U RNase inhibitor (Cat# N8080119, Thermo Scientific). The RT reaction mixture was incubated at 37 °C for 15 min to generate cDNA. Then, a 10 μl RT product was transferred into the 50 μl-basic RPA reaction mixture, which contains 29.5 μl rehydration buffer, one freeze-dried RPA reaction pellet (Cat# TABAS03KIT, TwistDx), 0.5 μM RT-RPA forward and reverse primer mix, and 14 mM MgOAc (last added to initiate the reaction). The RPA reaction mixture was incubated at 37 °C for another 15 min.

The following actions were taken to avoid the possible cross-contamination and environmental contamination: 1), the RT and RPA reactions were carried out at different biosafety cabinets, and the tubes of each step products were not opened unless cooling them off and centrifugation; 2), a nucleic acid scavenger, Sani-Cide EX3 (Cat# 42048–4, Guangzhou Smosnow Health), was used to remove the residual nucleic acid molecules in air or on the surfaces of the equipment or reagent packages before and after each reaction test.

2.2. CRISPR trans-cleavage assay for fluorescence-based and lateral-flow readouts

Briefly, a 100 μl volume basic CRISPR reaction mixture was used with 1 × *Lba*Cas12a buffer, 5 μl RT-RPA product, 0.2 μM *Lba*Cas12a (Cat# M0653T, New England Biolabs), 0.6 μM crRNA, 10 μM $MgCl_2$, 10 nM fluorophore (FAM)-quencher (BHQ1) ssDNA probe (FQ-ssDNA, Sangon Biotech) for the fluorescence-based detection, or 200 nM FTIC-Biotin ssDNA probe (FB-ssDNA, Zoonbio Biotechnology, Nanjing, China) for the lateral flow-based detection.

For the fluorescence-based readout, a 96-well plate containing 100 μl reaction mixture was incubated at 37 °C using the Cytation 5 Mul-Mode Reader (BioTek, VT, USA). Usually, a 60-min monitoring was used with an interval time of 30 s. The fluorescence excitation and emission wavelength were set as 485 nm and 520 nm, respectively. The relative fluorescence intensity (F/F_0) was calculated as the fluorescence signal relative to the starting signal. Generally, the fluorescence signals at the 30 min-reactions were quantified as F_{30}/F_0. In this study, $(F_{30}/F_0)_{Sample}$ / $(F_{30}/F_0)_{NC} \geq 1.2$ indicates the positive result while $(F_{30}/F_0)_{Sample}$ / $(F_{30}/F_0)_{NC} < 1.2$ indicates the negative result.

For the lateral flow readout, a 100 μl-reaction mixture was incubated in an Eppendorf tube at 37 °C for 30 min. Then, the HybriDetect strip (Milenia Biotec, Giessen, Germany) was placed into the Eppendorf tube, and the C-line and/or T-line were visualized and stabilized in ~2 min. The relative greyness of the T-line (G) was quantified using ImageJ. We used the same batched strip loaded with RNase-free water as the negative control (NC). In this study, we assumed that the G_{Sample} / $G_{NC} \geq 1.5$ of T-line indicates the positive result while G_{Sample} / $G_{NC} < 1.5$ of T-line indicates the negative result. Due to the incomplete digestion of FB-ssDNA, most positive test results displayed two lines (T-line and C-line) on the strips.

2.3. Validation of RRCd in detection and discrimination of clinical samples

To evaluate the performance of RRCd on SARS-CoV-2 clinical samples, a total of 194 swabs were collected at SITHC from March 3rd and to October 29th 2021 and were used to perform the RRCd assay. Both lateral-flow and fluorescence-based readouts were recorded. A total of 86 clinical samples were used to detect SARS-CoV-2 by targeting *E* gene and *S* gene, and a total of 108 clinical samples were used to detect and discriminate the SARS-CoV-2 VOCs by targeting *S* gene 501 or 478. The RRCd results were analyzed and compared with the results of RT-qPCR and genome sequencing.

More experimental details can be found at Supplementary Materials.

3. Results and discussion

3.1. Technical route of RRCd assay

The CRISPR-*Lb*Cas12a-based nucleic acid test platform HOLMES [17] was chosen as the starting core to design the technical route for RRCd (Fig. 1 and Fig. S1). Different from the previous methods [10,11,18], RRCd combines the advantages of high sensitivity of RT-RPA [19] and high specificity of CRISPR system [7] (Table S2). More importantly, RRCd uses the Cas protein of Cas12a, which possesses a greater specificity and a lower mismatch tolerance in comparison with Cas9 and Cas13 to the nucleic acid template [7], making it more suitable for genotyping of viral variants. We conducted a two-step RT-RPA amplification on SARS-CoV-2 genes to provide adequate double-stranded DNA (dsDNA) for the following CRISPR recognition system (Fig. 1, II). By designing specific crRNA, Cas12a recognizes and *cis*-cleaves the dsDNA templates of SARS-CoV-2 or its variants. Meanwhile, the formation of the ternary complex of Cas12a-crRNA-dsDNA activates the *trans*-activity of Cas12a, which leads to the cleavage of the non-targeted single--stranded DNA (ssDNA) probe in the system (Fig. 1, III). The results of

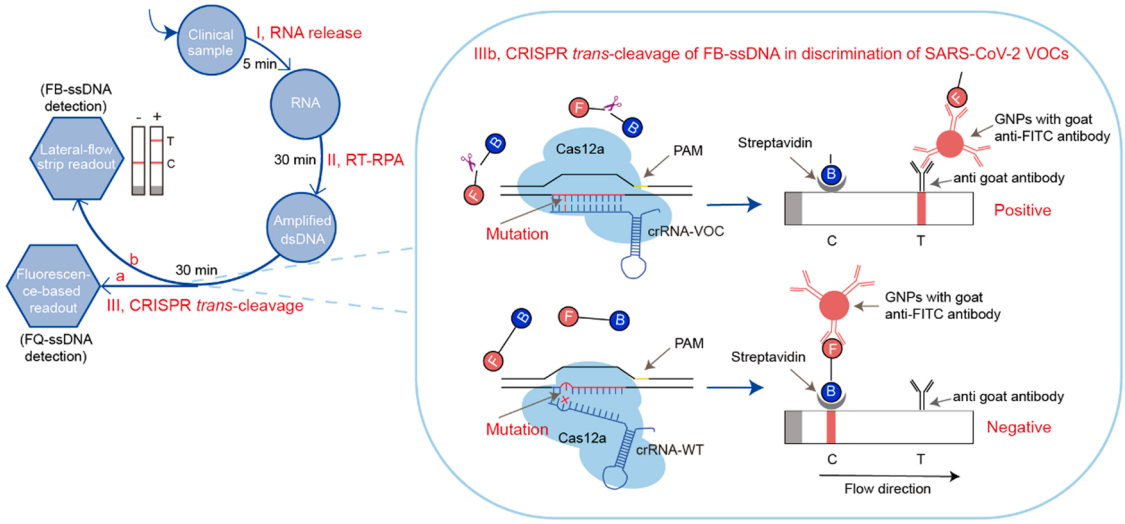


Fig. 1. Detection and discrimination of SARS-CoV-2 VOCs by RRCd. Schematic overview of RRCd workflow. (I) SARS-CoV-2 samples were released by automatic extraction (~ 10 min) or using RNA release chemical agents without extraction (~ 5 min). (II) The viral RNA was reverse transcribed into the dsDNA and amplified by RPA. (III) Cas12a was guided to target the dsDNA by the specific crRNA, thereby activated its *trans*-cleavage activity to the ssDNA probes in the system. The results could be quantified by fluorescence detection of the cleaved FQ-ssDNA (III a), or visualized by lateral-flow strip using the FB-ssDNA probe (III b). RRCd in discrimination of SARS-CoV-2 VOCs with lateral-flow readout is highlighted on the right panel. The target gene was shown as the template, and it was detected by either crRNA-VOC or crRNA-WT, leading to the positive (upper right panel) or negative (lower right panel) test result, respectively. Due to the FB-ssDNA probes are not 100% cleaved by Cas12a in the positive reaction system, there usually has a visible C-line (C) in the positive test results. dsDNA, double-strand DNA; ssDNA, single-strand DNA; FQ, fluorophore (FAM)-quencher (BHQ1); FB, FITC-Biotin; PAM, protospacer adjacent motif; VOC, variant of concern; WT, wild type; GNP, gold nanoparticle; gt, goat.

RRCd could be quantified directly by fluorescence detection of the fluorophore-quencher ssDNA (FQ-ssDNA) (Fig. 1, IIIa) or captured by lateral-flow strip using the FITC-Biotin ssDNA (FB-ssDNA) (Fig. 1, IIIb).

3.2. The specificity analyses of RRCd assay

Representative mutations in spike (S) protein can be used for genotyping of the SARS-CoV-2 lineages (Fig. S2). By screening optimal RT-RPA primers (Fig. S3) and crRNAs (Fig. S4) that target to the S protein encoding gene, RRCd was readily applied for the detection and discrimination of SARS-CoV-2 mutations (Fig. 2A-F). These include the first reported Alpha and Beta mutation N501Y [20] (Figs. 2A and 2B), the recent reported T478K on Delta and Omicron VOCs [21] (Figs. 2C and 2D), and the small deletion ΔH69-V70 on Alpha and Omicron VOCs [22] (Figs. 2E and 2F). The N501Y mutation in the receptor-binding domain (RBD) of S protein was reported to cause an increased transmission and infectivity of SARS-CoV-2 [23]. The T478K in the RBD is also involved in higher transmissibility by increasing the affinity to the human ACE2 receptor [21], while the deletion of H69V70 at the N-terminal domain is shown to allow the virus to replicate more efficiently [22].

Our test results were demonstrated by both the fluorescence-based and lateral-flow readouts, representing the *trans*-cleavage activity of Cas12a [7,16] (Fig. 2A-F). Additionally, we confirmed this specific cleavage by leveraging polyacrylamide gel electrophoresis analyses representing the Cas12a *cis*-cleavage activity [7] (Fig. S5A-C). Moreover, we showed that RRCd can be used for the discrimination of SARS-CoV-2 from other phylogenetic related viruses (Fig. S6).

3.3. The detection limit of RRCd

To determine the limit of detection (LoD) of RRCd, we built a standard curve to dissect the correspondences between the viral copy numbers and the C_t values using SARS-CoV-2 pseudovirus (Fig. S7). The C_t values of each dilution were measured using RT-qPCR targeting *N* gene or *ORF1ab* gene to mimic the clinical C_t ranges. Despite showing distinct kinetics, the fluorescence-based readouts revealed that the LoDs of all the targeted regions (*E* gene, N501, Y501, T478, and K478 of *S* gene) were ~10 copies per reactions, corresponding to a C_t value of 35 in the RT-qPCR assay (Fig. 3). The fluorescence results from a 30-min CRISPR reaction suggested that the detection sensitivity of N501 is a slightly higher than that of Y501 (Figs. 3B and 3C), while the detection sensitivity of T478 is a slightly lower than that of K478 (Figs. 3D and 3E). It is worth noting that the detection sensitivity of the lateral-flow readouts is 2–10 folds lower than that of the fluorescence-based readouts (Fig. 3), in consistent with the previous reports [11]. The detection of Y501 and K478 was shown to be the most sensitive when using the lateral-flow readout, with the LoDs of ~10 copies per reactions (Fig. 3).

To avoid false-discriminative results, we further assessed the factors that may affect the detection sensitivity in RRCd, including the sample volume and probe inputs, the usage of RNase H, T4 gene 32 protein, Bsu DNA polymerase, RPA kits, and Mg^{2+}. We found the sample volume and the usage of T4 gene 32 protein [24] are the key factors affecting RRCd sensitivity mostly (Fig. S8).

3.4. Validation of RRCd in detection and discrimination of clinical samples

Based on the optimized procedures, we evaluated the performance of RRCd on detecting COVID-19 clinical samples isolated from nasopharyngeal and salivary swabs. In coordination with the scenario of POCT, our available samples were collected from Shanghai Customs where the susceptible patients were characterized as asymptomatic and with low virus load (Fig. S9 and Table S1). To minimize the cognitive bias, all information of the clinical samples was confidential to study staff before the detection.

A validation study of SARS-CoV-2 detection was conducted on a total of 86 clinical samples (44 RT-qPCR-verified positive samples and 42 RT-qPCR-verified negative samples). Both *E* gene and *S* gene were used as the targeted sequences to acquire the double-checked detection results (Fig. 4 and Fig. S10). RRCd identified all the positive samples with $C_t < 33$ through both lateral-flow and fluorescence-based readouts. In addition, 42 COVID-19 negative samples were all identified without false positive results from both readouts. Samples beyond the C_t value of

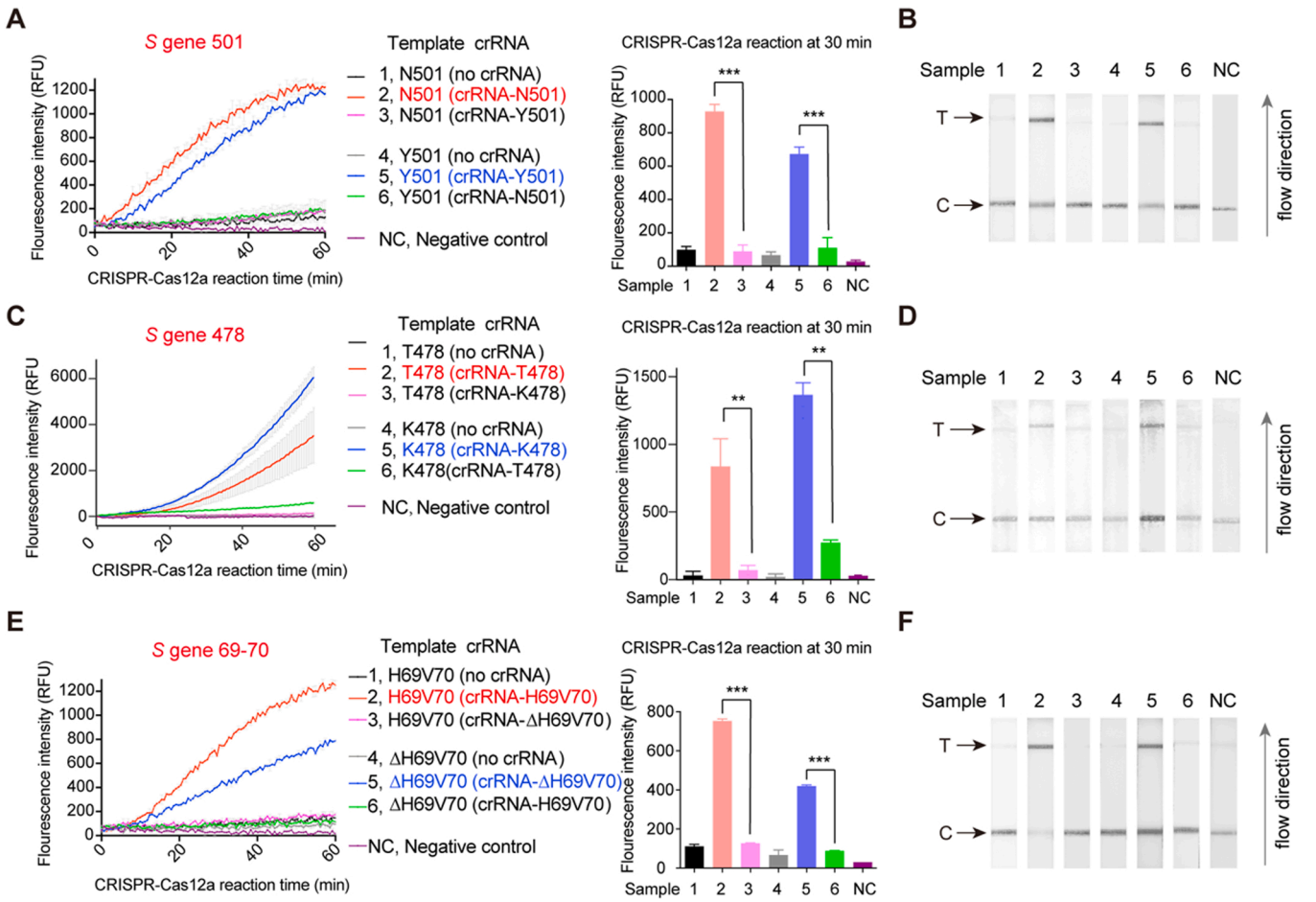


Fig. 2. The specificity of RRCd in detection of SARS-CoV-2 VOCs. A. Specificity analysis of RRCd in detection of SARS-CoV-2 *S* gene 501, using fluorescence-based readouts. The dsDNA derived from pseudovirus *S* gene N501 or Y501 was incubated with Cas12a, FQ-ssDNA, and distinct crRNA at 37 °C, and the corresponding fluorescence signal was recorded over 60 min (left panel) and quantified at 30 min (right panel). Data are presented as the mean ± S.D. (n = 3). * ** , $P < 0.001$ by student's *t* test. RNase-free water was used as the negative control (NC). RFU, relative fluorescence units. B. Specificity analysis of RRCd using lateral-flow readouts. The samples analyzed were the same as those in panel B. The reactions were conducted at 37 °C for 30 min before the mixtures were transferred onto the strips, using FB-ssDNA probe instead of FQ-ssDNA. The relative greyness (G) of strip bands was quantified using ImageJ. In this study, G_{Sample} / G_{NC} of the T band ≥ 1.5 indicates positive. C, D. Specificity analysis of RRCd in detection of SARS-CoV-2 *S* gene 478. E, F. Specificity analysis of RRCd in detection of SARS-CoV-2 *S* gene 69–70.

32 were more likely to be detected by targeting the *E* gene ($C_t \leq 35$, 100% detected) than the *S* gene (Fig. 4). The detection sensitivity of these results was comparable to the RT-LAMP-Cas12 based DETECTR [10] and the RT-RPA-Cas13 based SHERLOCK [11], showing a 99% positive predictive agreement (PPA) and 100% negative predictive agreement (NPA) in both readouts ($C_t < 33$) (Table 1).

We next evaluated the performance of RRCd on discrimination of SARS-CoV-2 mutations. The 501 position of *S* gene was used as a target to detect SARS-CoV-2 VOCs, such as the Alpha, Beta, Gamma, and Omicron [20]. A total of 68 clinical samples, consisting of 28 genome-sequencing-verified N501 samples and 19 genome-sequencing-verified Y501 samples, were collected from March 3rd to April 10th 2021 at Shanghai Customs. RRCd discriminated all the variants from samples with a $C_t < 32$, either using lateral-flow readouts or fluorescence-based readouts (Fig. 5A and Fig. S11). However, the discrimination ability decreased strikingly when testing the samples with C_t values beyond 33, which is possibly due to the relatively high LoD of *S* gene 501 as shown above (Fig. 3). The 478 position of *S* gene was used as a target to identify Delta and Omicron VOCs [21]. A total of 40 clinical positive samples, consisting of 7 genome-sequencing-verified T478 samples and 14 genome-sequencing-verified K478 samples, were collected from May 27th and October 29th 2021. RRCd was able to discriminate all the variants targeting the *S* gene 478. Moreover, RRCd displayed a relatively higher sensitivity in detecting the position of 478 than that of 501, with the C_t value reaching 34. The detection results were confirmed by both readouts with 0% false-discriminant rates (Fig. 5B and S12). Taken together, these data show that a total of 89% positive predictive agreement and 100% negative predictive agreement in 194 clinical samples, demonstrating RRCd detect and discriminate the SARS-CoV-2 mutations accurately and sensitively (Table 1).

Moreover, SARS-CoV-2 detection using direct lysing the clinic samples without RNA extraction and purification was demonstrated (Fig. S13). Although a relatively small sample size was used, these results indicate that the whole process of RRCd including the RT-RPA amplification and the lateral-flow detection is independent of electrical devices, which may facilitate the development of POCT products in the future.

4. Conclusions

In this study, an RRCd method aiming to detection and discrimination of SARS-CoV-2 mutations has been developed. RRCd completed in ~1 h and displayed a sensitivity down to 10 copies per reaction. By targeting and identifying the representative N501Y, T478K and ΔH69-V70 mutations, RRCd discriminated the mutations on COVID-19 samples related to SARS-CoV-2 VOCs. The method was validated in 194 clinical COVID-19 samples, with 99% PPA and 100% NPA for the samples of $C_t < 33$ through both the fluorescence and the lateral-flow

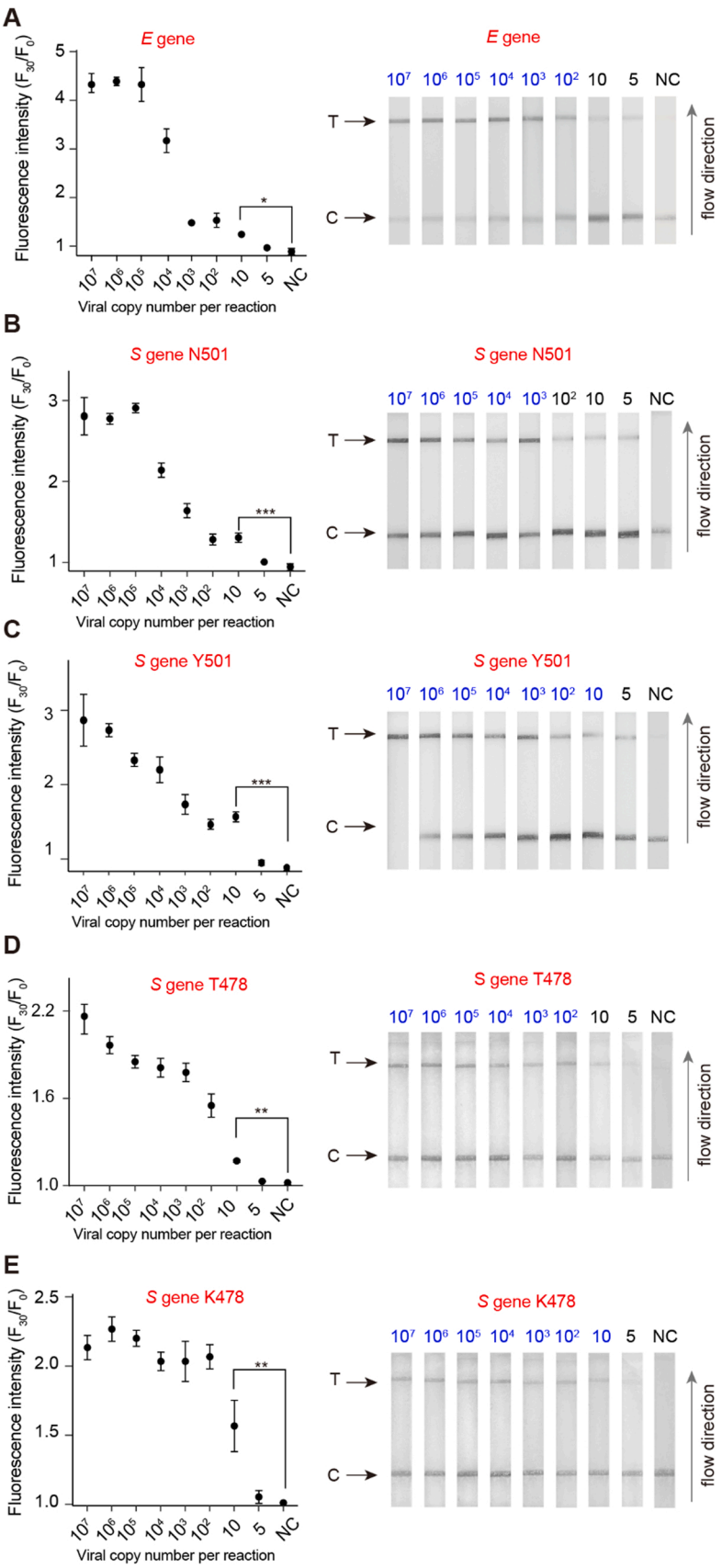


Fig. 3. The detection limit of RRCd for SARS-CoV-2 VOCs. The detection limit of the targeted regions in VOCs were determined by using 10^7, 10^6, 10^5, 10^4, 10^3, 10^2, 10 and 5 copies of pseudovirus RNA per reaction, respectively. The dsDNA derived from the pseudovirus RNA was incubated with Cas12a, ssDNA probe, and crRNA at 37 °C for 30 min. The fluorescence signal at the 30 min-reaction was quantified (left panel). The positive samples of lateral-flow readouts (right panel) are indicated as blue by the T-line quantification as described. Data are presented as mean ± S.D. from at least three independent experiments. For the dilutions with 10 and 5 copies per reaction, at least five independent experiments were conducted. A. LoD determination of RRCd for *E* gene. B-E. LoD determinations of RRCd for N501 (B), Y501 (C), T478 (D) and K478 (E) in *S* gene, respectively. * , $P < 0.05$; * *, $P < 0.01$; * ** , $P < 0.001$. NC, negative control using the RNase-free water.

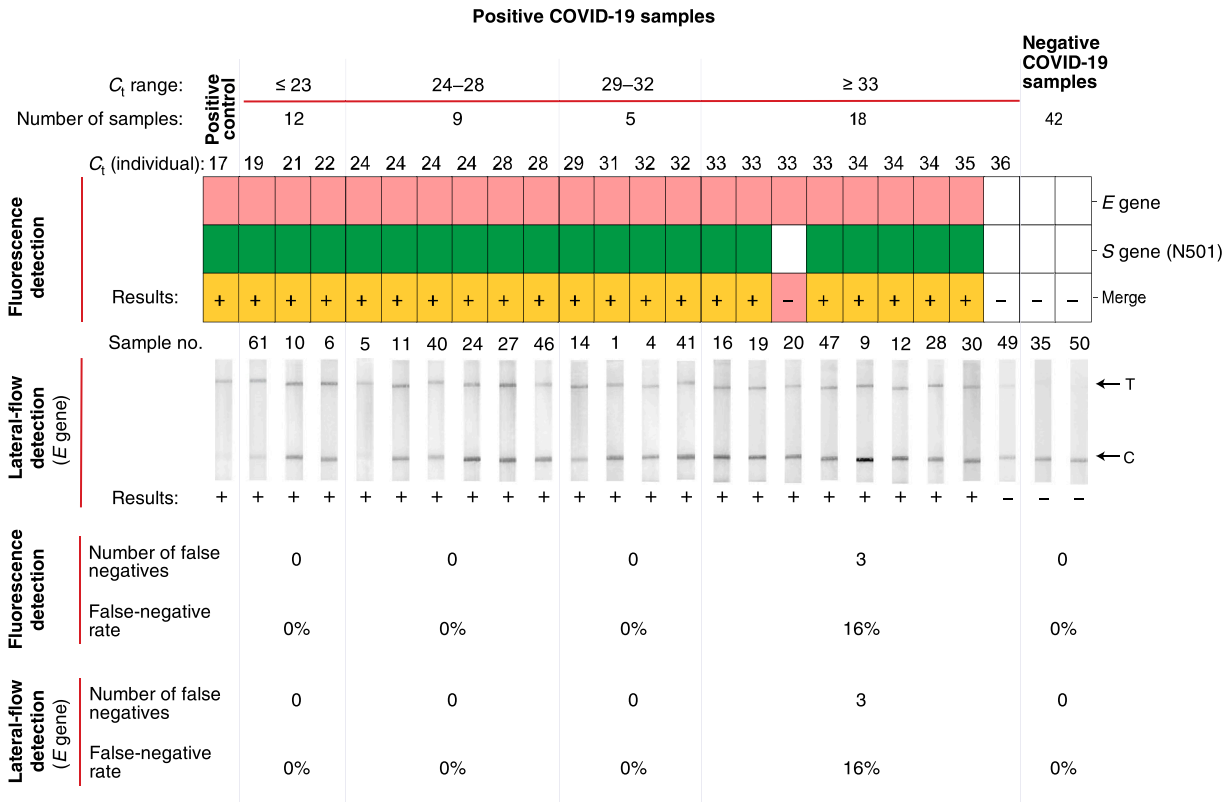


Fig. 4. Validation of RRCd in detection of 86 RT-qPCR-verified clinical samples. A double-checked detection (*E* gene and *S* gene) was executed for the clinical samples by RRCd. Representatives of fluorescence-based readouts and lateral-flow readouts of the positive samples as well as the negative samples are shown on the middle of the panel. Both *E* gene and *S* gene (N510) were used as the targeted sequences in fluorescence-based readouts. The light red and green indicate the positive detection results of *E* gene and *S* gene (N501), respectively, while the orange represents the double-checked positive result. The white indicates the negative result. Only the lateral-flow results of *E* gene are shown. + , positive;–, negative or indistinguishable. The analyses of the detection results are shown as the number of false negatives and the false-negative rate for each C_t range on the bottom of the panel. The SARS-CoV-2 pseudovirus was used as the positive control. The full dataset is shown in Fig. S10.

Table 1
Predictive agreements of RRCd in detection of clinical samples.

	RRCd results	RT-qPCR-verified positive samples		RT-qPCR-verified negative samples
		$C_t < 33$	$C_t \geq 33$	
Fluorescence-based readout	Positive	74 (true positive)	24 (true positive)	0 (false positive)
	Negative	1 (false negative)	13 (false negative)	82 (true negative)
	Total	75	37	82
	PPA/NPA	99%	65%	100%
	Total PPA/NPA	89%		100%
Lateral-flow readout	Positive	74 (true positive)	23 (true positive)	0 (false positive)
	Negative	1 (false negative)	14 (false negative)	82 (true negative)
	Total	75	37	82
	PPA/NPA	99%	62%	100%
	Total PPA/NPA	88%		100%

In total, 194 clinical samples including 112 positive samples and 82 negative samples were analyzed by RRCd with both fluorescence-based and lateral-flow readouts. PPA, positive predictive agreement; NPA, negative predictive agreement.

readouts (Table 1). RRCd also has the potential to be easily adapted to detect novel mutations on SARS-CoV-2 or other epidemic viruses by designing the new RT-RPA primers and crRNAs, without changing the subsequent detection procedures and ssDNA probes (Fig. 1 and Fig. S1). Moreover, for those targeted DNAs without the proper PAM, our RRCd could introduce an exogenous 5' TTTV PAM by designing the RPA primers, which increases the adaptability of this method to target broader sites.

Although displaying a high adaptability and was validated by large clinical samples, RRCd assay could only be used to detect known sequences or mutations of viruses, and it will never replace the whole genome sequencing in discovering new viral mutations. Moreover, RRCd is not able to detect all the mutations as genome sequencing since more and more mutations emerging in SARS-CoV-2. These new mutations will either increase the detection dimensions because more crRNAs are needed, or reduce the specificity of crRNA recognitions due to the undesirable mutations may happen and affect the crRNA binding sites. In addition, the LoDs of RRCd were usually higher in discriminating viral variants than detecting the wild-type sequences, and were varied between the detection of distinct mutations. These therefore require that the viral genome sequences and the optimal RT-RPA primers and crRNAs be analyzed and screened in advance.

Therefore, the application scenarios of RRCd could be on site detection (*e.g.*, self-testing), or where the power access is limited (*e.g.*, underdeveloped areas), or when quick turnaround times are needed (*e.g.*, hospital emergency). Further modification of this method to meet the requirements of POCT products is still needed.

CRediT authorship contribution statement

Guiyue Tang: Conceptualization, Data curation, Writing – review & editing. **Zilong Zhang**: Data curation, Funding acquisition, Resources.

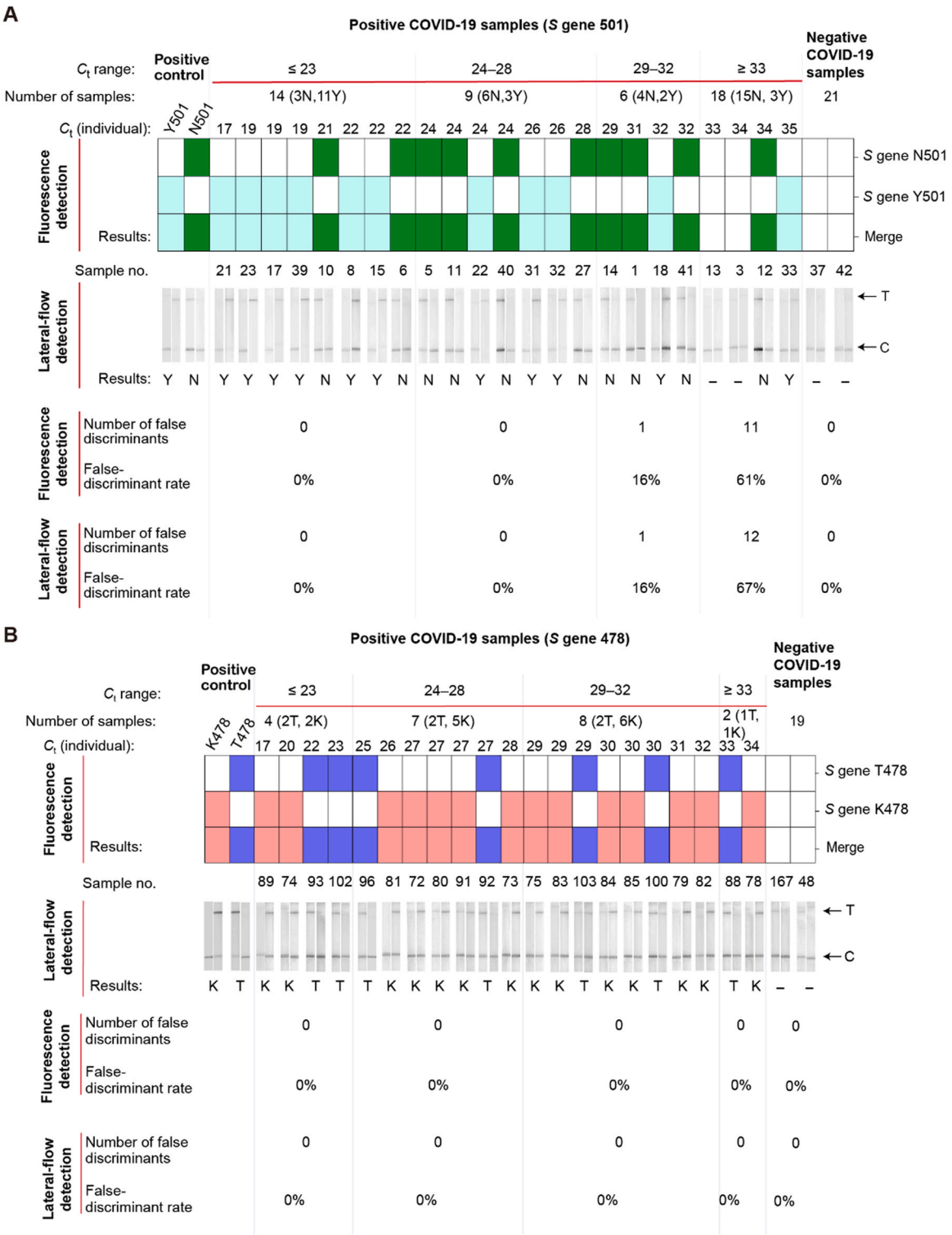


Fig. 5. Validation of RRCd in detection and discrimination of 108 genome-sequencing-verified clinical samples. Discrimination of SARS-CoV-2 *S* gene 501 variants in clinical samples. The total number of clinical samples in each C_t range are shown on the top of the panel and the corresponding genome-sequencing-verified mutations are displayed in the brackets (For details please see Table S1). In total, 47 positive samples (C_t range of 13–35) and 21 negative samples were detected. The *S* gene 501 variants were discriminated by crRNA-N501 (green) and crRNA-Y501 (light blue) using fluorescence-based readouts. In addition, the lateral-flow readouts are displayed in the middle of the panel using crRNA-N501 (left) and crRNA-Y501 (right). N, N501; Y, Y501; –, negative or indistinguishable. The analysis results are shown as the number of false discriminants and the false-discriminant rate for each C_t range on the bottom of the panel. B. Discrimination of SARS-CoV-2 *S* gene 478 variants in clinical samples. In total, 21 positive samples (C_t range of 17–34) and 19 negative samples were detected. The *S* gene 478 variants were discriminated by crRNA-T478 (blue) and crRNA-K478 (pink) by fluorescence readouts. The lateral-flow readouts using crRNA-T478 (left) and crRNA-K478 (right) are displayed on the below. T, T478; K, K478;–, negative or indistinguishable. The corresponding SARS-CoV-2 pseudoviruses were used as the positive controls. The full datasets for panel a and b are shown in Fig. S11 and Fig. S12, respectively.

Wei Tan: Conceptualization, Writing – review & editing. **Fei Long**: Data curation, Formal analysis. **Jingxian Sun**: Investigation. **Yingying Li**: Investigation. **Siwei Zou**: Investigation. **Yujiao Yang**: Investigation. **Kezhu Cai**: Investigation. **Shenwei Li**: Investigation. **Zhiyi Wang**: Investigation. **Jiakun Liu**: Formal analysis. **Guobing Mao**: Formal analysis. **Yingxin Ma**: Formal analysis. **Guo-Ping Zhao**: Conceptualization, Funding acquisition, Resources. **Zhen-Gan Tian**: Conceptualization, Funding acquisition, Resources. **Wei Zhao**: Conceptualization, Supervision, Funding acquisition, Resources, Writing – review & editing.

Declaration of Competing Interest

The authors declare that they have no known competing financial interests or personal relationships that could have appeared to influence the work reported in this paper.

Data Availability

No data was used for the research described in the article.

Acknowledgments

We are grateful to Prof. Xian-En Zhang for generously providing the pseudovirus, and Prof. Hang Dai and Dr. Xiaonan Yang for discussing on this project. This study was supported by the National Key Research and Development Program of China (2019YFA0904003, 2020YFA0909100), the Strategic Priority Research Program of the Chinese Academy of Sciences, China (XDB38020300), the Guangdong Basic and Applied Basic Research Foundation (2021A1515012511), and the General Administration of Customs Project (2020HK003).

Conflict of interest

G.T., W.T., G.P.Z. and W.Z. are co-inventors on patent applications filed by Shenzhen Institutes of Advanced Technology relating to the work in this manuscript. The remaining authors declare no conflict of interest.

Appendix A. Supporting information

Supplementary data associated with this article can be found in the online version at doi:10.1016/j.snb.2023.133433.

References

[1] K. Tao, P.L. Tzou, J. Nouhin, R.K. Gupta, T. de Oliveira, S.L.Kosakovsky Pond, et al., The biological and clinical significance of emerging SARS-CoV-2 variants, Nat. Rev. Genet 22 (2021) 757–773, https://doi.org/10.1038/s41576-021-00408-x.

[2] B.B. Oude Munnink, N. Worp, D.F. Nieuwenhuijse, R.S. Sikkema, B. Haagmans, R. A.M. Fouchier, et al., The next phase of SARS-CoV-2 surveillance: real-time molecular epidemiology, Nat. Med 27 (2021) 1518–1524, https://doi.org/10.1038/s41591-021-01472-w.

[3] A. Crits-Christoph, R.S. Kantor, M.R. Olm, O.N. Whitney, B. Al-Shayeb, Y.C. Lou, et al., Genome sequencing of sewage detects regionally prevalent SARS-CoV-2 variants, mBio 12 (2021), https://doi.org/10.1128/mBio.02703-20.

[4] M. Kumar, S. Gulati, A.H. Ansari, R. Phutela, S. Acharya, M. Azhar, et al., FnCas9-based CRISPR diagnostic for rapid and accurate detection of major SARS-CoV-2 variants on a paper strip, eLife 10 (2021), https://doi.org/10.7554/eLife.67130.

[5] C.B.F. Vogels, M.I. Breban, I.M. Ott, T. Alpert, M.E. Petrone, A.E. Watkins, et al., Multiplex qPCR discriminates variants of concern to enhance global surveillance of SARS-CoV-2, PLoS Biol. 19 (2021), https://doi.org/10.1371/journal.pbio.3001236.

[6] T. Peto, COVID-19: rapid antigen detection for SARS-CoV-2 by lateral flow assay: a national systematic evaluation of sensitivity and specificity for mass-testing, EClinicalMedicine 36 (2021), 100924, https://doi.org/10.1016/j.eclinm.2021.10092.

[7] J.S. Chen, E. Ma, L.B. Harrington, M. Da Costa, X. Tian, J.M. Palefsky, et al., CRISPR-Cas12a target binding unleashes indiscriminate single-stranded DNase activity, Science 360 (2018) 436–439, https://doi.org/10.1126/science.aar6245.

[8] J. Joung, A. Ladha, M. Saito, N.G. Kim, A.E. Woolley, M. Segel, et al., Detection of SARS-CoV-2 with SHERLOCK one-pot testing, N. Engl. J. Med 383 (2020) 1492–1494, https://doi.org/10.1056/NEJMc2026172.

[9] P. Fozouni, S. Son, M. Diaz de Leon Derby, G.J. Knott, C.N. Gray, M.V. D'Ambrosio, et al., Amplification-free detection of SARS-CoV-2 with CRISPR-Cas13a and mobile phone microscopy, Cell 184 (2021) 323–333 e9, https://doi.org/10.1016/j.cell.2020.12.001.

[10] J.P. Broughton, X. Deng, G. Yu, C.L. Fasching, V. Servellita, J. Singh, et al., CRISPR-Cas12-based detection of SARS-CoV-2, Nat. Biotechnol. 38 (2020) 870–874, https://doi.org/10.1038/s41587-020-0513-4.

[11] M. Patchsung, K. Jantarug, A. Pattama, K. Aphicho, S. Suraritdechachai, P. Meesawat, et al., Clinical validation of a Cas13-based assay for the detection of SARS-CoV-2 RNA, Nat. Biomed. Eng. 4 (2020) 1140–1149, https://doi.org/10.1038/s41551-020-00603-x.

[12] Y. Wang, Y. Zhang, J. Chen, M. Wang, T. Zhang, W. Luo, et al., Detection of SARS-CoV-2 and its mutated variants via CRISPR-Cas13-based transcription amplification, Anal. Chem. 93 (2021) 3393–3402, https://doi.org/10.1021/acs.analchem.0c04303.

[13] B. Ning, B.M. Youngquist, D.D. Li, C.J. Lyon, A. Zelazny, N.J. Maness, et al., Rapid detection of multiple SARS-CoV-2 variants of concern by PAM-targeting mutations, Cell Rep. Methods 2 (2022), 100173, https://doi.org/10.1016/j.crmeth.2022.100173.

[14] H. de Puig, R.A. Lee, D. Najjar, X. Tan, L.R. Soeknsen, N.M. Angenent-Mari, et al., Minimally instrumented SHERLOCK (miSHERLOCK) for CRISPR-based point-of-care diagnosis of SARS-CoV-2 and emerging variants, Sci. Adv. 7 (2021), https://doi.org/10.1126/sciadv.abh2944.

[15] F. Teng, L. Guo, T. Cui, X.G. Wang, K. Xu, Q. Gao, et al., CDetection: CRISPR-Cas12b-based DNA detection with sub-attomolar sensitivity and single-base specificity, Genome Biol. 20 (2019) 132, https://doi.org/10.1186/s13059-019-1742-z.

[16] S.Y. Li, Q.X. Cheng, J.K. Liu, X.Q. Nie, G.P. Zhao, J. Wang, CRISPR-Cas12a has both *cis*- and *trans*-cleavage activities on single-stranded DNA, Cell Res 28 (2018) 491, https://doi.org/10.1038/s41422-018-0022-x.

[17] S.Y. Li, Q.X. Cheng, J.M. Wang, X.Y. Li, Z.L. Zhang, S. Gao, et al., CRISPR-Cas12a-assisted nucleic acid detection, Cell Disco 4 (2018) 20, https://doi.org/10.1038/s41421-018-0028-z.

[18] X. Ding, K. Yin, Z. Li, R.V. Lalla, E. Ballesteros, M.M. Sfeir, et al., Ultrasensitive and visual detection of SARS-CoV-2 using all-in-one dual CRISPR-Cas12a assay, Nat. Commun. 11 (2020) 4711, https://doi.org/10.1038/s41467-020-18575-6.

[19] I.M. Lobato, C.K. O'Sullivan, Recombinase polymerase amplification: basics, applications and recent advances, Trends Anal. Chem. 98 (2018) 19–35, https://doi.org/10.1016/j.trac.2017.10.015.

[20] H. Tegally, E. Wilkinson, M. Giovanetti, A. Iranzadeh, V. Fonseca, J. Giandhari, et al., Detection of a SARS-CoV-2 variant of concern in South Africa, Nature 592 (2021) 438–443, https://doi.org/10.1038/s41586-021-03402-9.

[21] S. Kumar, T.S. Thambiraja, K. Karuppanan, G. Subramaniam, Omicron and Delta variant of SARS-CoV-2: a comparative computational study of spike protein, J. Med Virol. 94 (2022) 1641–1649, https://doi.org/10.1002/jmv.27526.

[22] B. Meng, S.A. Kemp, G. Papa, R. Datir, I. Ferreira, S. Marelli, et al., Recurrent emergence of SARS-CoV-2 spike deletion H69/V70 and its role in the Alpha variant B.1.1.7, Cell Rep. 35 (2021), 109292, https://doi.org/10.1016/j.celrep.2021.109292.

[23] Y. Liu, J. Liu, K.S. Plante, J.A. Plante, X. Xie, X. Zhang, et al., The N501Y spike substitution enhances SARS-CoV-2 infection and transmission, Nature 602 (2022) 294–299, https://doi.org/10.1038/s41586-021-04245-0.

[24] C. Villalva, C. Touriol, P. Seurat, P. Trempat, G. Delsol, P. Brousset, Increased yield of PCR products by addition of T4 gene 32 protein to the SMART PCR cDNA synthesis system, 6, Biotechniques 31 (2001) 81–83, https://doi.org/10.2144/01311st04.

Guiyue Tang is a research assistant at Shenzhen Institutes of Advanced Technology, Chinese Academy of Sciences. She is mainly interested in CRISPR technology.

Zilong Zhang is an assistant professor at Shanghai International Travel Healthcare Center, Shanghai Customs District P. R. China. He is mainly interested in the molecular diagnosis of infectious microorganisms.

Wei Tan is an assistant professor at Shenzhen Institutes of Advanced Technology, Chinese Academy of Sciences. His main research interests are synthetic cell biology and liquid-liquid phase separation in biology.

Fei Long is an assistant professor at Shenzhen Institutes of Advanced Technology, Chinese Academy of Sciences. He is mainly interested in biochemistry.

Jingxian Sun is an assistant professor at Shenzhen Institutes of Advanced Technology, Chinese Academy of Sciences. His current research field focuses on the genetic engineering of the gut microbiome.

Yingying Li is an assistant professor at Shenzhen Institutes of Advanced Technology, Chinese Academy of Sciences. Her current research field focuses on microbial cell polarity.

Siwei Zou is an assistant professor at Shenzhen Institutes of Advanced Technology, Chinese Academy of Sciences. His research field is the molecular evolution of the sirtuin protein.

Yujiao Yang is a Ph.D. student at CAS Center for Excellence in Molecular Plant Sciences, Chinese Academy of Sciences. Her main research interests are synthetic cell biology and post-translation modification.

Kezhu Cai is a visiting student at Shenzhen Institute of Advanced Technology, Chinese Academy of Sciences. He majored in bioinformatics.

Shenwei Li is an assistant professor at Shanghai International Travel Healthcare Center, Shanghai Customs District P. R. China. She is mainly interested in molecular detection.

Zhiyi Wang is an assistant professor at Shanghai International Travel Healthcare Center, Shanghai Customs District P. R. China. She is mainly interested in molecular detection.

Jiakun Liu is an assistant professor at Shenzhen Institutes of Advanced Technology, Chinese Academy of Sciences. He majored in synthetic biology.

Guobin Mao is an associate professor at Shenzhen Institutes of Advanced Technology, Chinese Academy of Sciences. His research interests are focused on nano-biosensors, *in vitro* diagnosis, labeling and imaging of virus.

Yingxin Ma is an associate professor at Shenzhen Institutes of Advanced Technology, Chinese Academy of Sciences. Her research interests are focused on fluorescence nano-sensors, diagnosis and treatment of tumor, labeling and imaging of virus.

Guo-Ping Zhao is a professor at Shenzhen Institutes of Advanced Technology, Chinese Academy of Sciences. He is a member of the Chinese Academy of Sciences (CAS) (elected in 2005), a fellow of the Third World Academy of Sciences (elected in 2011), and the honorary president of the Chinese Society for Microbiology (since 2012). His current research interests include biomedical big data and the synthetic biology of microorganisms.

Zhen-Gan Tian a professor of Shanghai International Travel Healthcare Center, Shanghai Customs District P. R. China. His current research interests include CRISPR technology and molecular diagnosis.

Wei Zhao is an associate professor at Shenzhen Institutes of Advanced Technology, Chinese Academy of Sciences. His current research interests include synthetic cell biology and microbiome.